Fast pyrolysis of wheat straw – Improvements of operational stability in 10 years of bioliq® pilot plant operation

Andreas Niebel [a]*, Axel Funke [a], Cornelius Pfitzer [a], Nicolaus Dahmen [a], Nicole Weih [a], Daniel Richter [a], Bernd Zimmerlin [b]

[a] Institute of Catalysis Research and Technology (IKFT), Karlsruhe Institute of Technology, Hermann-von-Helmholtz-Platz 1, 76344 Eggenstein-Leopoldshafen, Germany

[b] Institute for Technical Chemistry (ITC), Karlsruhe Institute of Technology, Hermann-von-Helmholtz-Platz 1, 76344 Eggenstein-Leopoldshafen, Germany

KEYWORDS: Fast pyrolysis, twin screw mixer reactor, wheat straw, bioliq process, biosyncrude, bio-oil, biomass to liquid (BtL), pilot plant operation

ABSTRACT: The bioliq® process developed at KIT aims at the conversion of lignocellulosic biomass into synthetic biofuels and chemicals. The process follows a two stage concept combining de-centralized pre-treatment of biomass via fast pyrolysis and centralized large scale gasification and synthesis. The process was specifically designed to convert ash-rich biomass residues, such as wheat straw, requiring special design features at least in the upstream processes. The 2 MW fast

pyrolysis pilot plant at Karlsruhe Institute of Technology (KIT) was operated with wheat straw from 2009 to 2018 and since then with miscanthus. A substantial increase from less than 5 tons wheat straw converted per test run in 2012 to more than 50 tons in 2018 was achieved. In total, up to 2018, more than 260 tons of wheat straw were converted into pyrolysis products within a total of 500 h of steady operation. Representative results of the product yields and properties were presented for test campaigns from 2015 to 2018 and compared to a process demonstration unit of the same design but with a downscale factor of 50 (10 kg/h). Mass yields from both plants are in good agreement and consistent with literature data. Experience from longer-term operation and major technical modifications made to improve the operational stability of the plant are described.

1. Introduction

Biomass residues are an increasingly popular resource for sustainable bioenergy production. On an energy basis, the amount of global harvest and processing residues from agriculture and forestry are of a comparable order of magnitude as the overall crop harvest, providing a significant and sustainable feedstock potential [1, 2]. During harvest and processing of agricultural crops various lignocellulosic residues such as cereal straw, corn stover and cobs, sunflower stalks, orchard pruning etc. are by-produced. Also, harvest and cultivation residues of forestry such as bark, tree tops and thinning as well as processing residues like saw dust, shavings and waste wood pieces may be utilized. Apart from its use as a material, wood is already widely utilized for bioenergy production mainly by combustion, but also by other thermochemical conversion processes such as pyrolysis or gasification. Heat from combustion is mostly used for domestic heating and cooking. While gasification at smaller scales is an established process for the generation of producer gas for direct heat or combined heat and power production, pyrolysis can target the production of different liquid and solid bioenergy carriers, depending on temperature and residence time applied.

Relatively mild conditions are applied for torrefaction, for example, to improve the quality of wood pellets; solid bio-coal is produced at higher temperatures mainly by slow pyrolysis to yield charcoal for energetic but also for material and chemical applications. The main product of fast pyrolysis is liquid bio-oil, suitable for direct use as heating oil and, after catalytic hydrotreatment, as a refinery-compatible feedstock.

A comprehensive overview of the current state of the art in fast pyrolysis regarding process fundamentals, technologies, feedstocks as well as of product yields and properties is given in the comprehensive reviews by R. Venderbosch and W. Prins [3] as well as by D. Meier et al. [4], both containing a valuable list of references. The technical development of fast pyrolysis processes is observed and frequently reported by the IEA Bioenergy Task 34 “Direct thermal liquefaction”. After around 40 years of intensive research and development work, fast pyrolysis plants are in commercial operation today. In Canada and the US, Ensyn (Canada) has provided its mature RTP technology to a number of commercially operated plants, partly in co-operation with companies such as Red Arrows or in the joint venture with Honeywell´s UOP, Envergent. Products focus on heating fuels and chemicals for the food industry. In Europe, the first, pre-commercial plant was commissioned by Fortum in 2013 in Joensuu, Finland capable for the production of 50,000 tons of fast pyrolysis bio-oil (FPBO) per year for heating purposes. The Valmet fast pyrolysis reactor is integrated into the combined heat and power plant of Fortum, making use of a license of VTT, the technical research center of Finland. Empyro BV has constructed a FP plant in Hengelo, The Netherlands, continuously producing around of 24,000 t/y of FPBO since 2015 using the rotating cone reactor technology developed by Biomass Technology Group BV (BTG) [5]. FPBO is co-fired with natural gas in the nearby dairy of FrieslandCampina. A new plant based on BTG´s

technology was recently commissioned in Finland. Other plants and projects can be found in the Pyrolysis Demoplant database of IEA TCP Bioenergy Task 34.

The most commonly used feedstock in commercial operation is wood, which is easily available on the market and leads to good-natured FPBOs. Due to its chemical composition and combustion behavior, crude FPBO cannot directly be used as motor fuel. In addition, it is practically not miscible with diesel, gasoline or other biofuels [6]. Quality improvements in bio-oil applications other than heating, such as the use as refinery feed, can be achieved by upgrading as reviewed by S. Xiu [7]. Upgrading typically aims at stabilization, deoxygenation, and eventually reduction of the molecular mass of bio-oil components. According to the desired application, a multistage hydrogenation process may become necessary [8, 9]. Char and non-condensable fuel gas are used in the process for heat generation and for the production of excess heat and electricity.

The aim of the fast pyrolysis process developed at KIT is focused on the production of a gasification fuel suitable for pressurized entrained flow gasification within the bioliq® BtL (biomass to liquids) process for the production of synthesis gas and subsequently of synthetic bio-fuels [10]. For this purpose, the FPBO is mixed with the by-produced char forming a liquid-like, viscous suspension, also referred to as biosyncrude, providing a higher heating value and more convenient handling, storage and transport compared to the original biomass. By doing so, a maximum of biocarbon from the biomass feedstock is maintained for further processing to liquid fuels. The bioliq® process was specifically designed for the use of ash-rich materials to access a large variety of biomass feedstock and, thus, a high mass potential. Therefore, the fast pyrolysis process as the first process step should be particularly able to convert different types of lignocellulosic biomass. The elementary composition of moist and ash-free lignocellulose is usually in a range around 50 wt.% carbon, 6 wt.% hydrogen and 44 wt.% oxygen and well

represented by the formula $C_1H_{1.45}O_{0.67}$ or simplified $C_3H_4O_2$. Wood contains only 0.5–2 wt.% of ash, while fast growing biomass like leaves or straw contains 5–10 wt.% ash, rice straw with 15–20 wt.% ash is an extreme example. Biomass for pyrolysis is usually dried to a water content below 15 wt.% allowing for feedstock storage without biological degradation. A higher protein content, e.g. in forage plants, causes negligible changes in the HHV (higher heating value), but increases the nitrogen content to 16 % of the protein weight. Fast pyrolysis of such materials may lead to significant changes in product distribution regarding the formation of liquids, solids, and gases. Specifically, ash constituents may lead to increased formation of reaction water, eventually leading to phase separation of the liquid condensate [11]. Therefore, a two-stage condensation system is installed in the bioliq® fast pyrolysis plant, which leads to a condensate rich in organics, and an aqueous condensate.

For around 10 years now, KIT's pilot plant has been operated with wheat straw as feedstock. This paper reports on the operating experience, methods for determining the mass and energy balance as well as yields and properties of products during this period. It is the first comprehensive publication with this scope and includes new results from test campaigns after 2015 [12, 13] as well as additional insights into operating experience compared to a previous report [14]. Detailed results on pilot plant operation are not frequently reported in literature, restricted by IPR and contracting issues of industrial partners usually involved in that stage of process development. This contribution addresses this problem by providing an in-depth pilot plant review for fast pyrolysis.

2. Process and methods

2.1 Fast pyrolysis process

Fast pyrolysis (FP) is characterized by rapid heating of the fine fuel particles by means of a hot heat carrier material, short gas residence times in the pyrolysis reactor and instant quenching of the pyrolysis vapors. In the bioliq® fast pyrolysis process, depicted in **Figure 1**, a twin-screw reactor is used to mix the straw particles 3–5 mm in size with an excess of 1 mm sand particles in a mass ratio of 10 to 20-fold at a reaction temperature of 500±20 °C and atmospheric pressure in the absence of oxygen. Gases and vapors are released; the vapor stream also contains most of the char, which is entrained as a dust of fines. By the pyrolysis reaction, the heat carrier cools by around 50 K and is then reheated and recirculated by hot flue gas in a lift pipe. For this purpose, hot flue gas is produced by natural gas combustion is used (in perspective, the non-condensable pyrolysis may be used instead). Char contained in the recycled sand is combusted by adjusting a certain oxygen excess in the gas burner and the resulting temperature is adjusted by moderation with steam. The hot flue gas passes a cyclone, an air preheater and a hot gas filter, before being flared off together with the non-condensable product gas from pyrolysis. Immediately downstream from the FP reactor, the entrained char particles are removed from the product gas stream with a hot cyclone still at reaction temperature of 500 °C. Rapid product recovery by cooling is essential to prevent further decomposition of condensable organic vapors. The organic vapors are condensed at around 85–90 °C by quench condensation via injection of cooled condensate, recirculated via a cooler. The volatile vapors are condensed after passing an electrostatic precipitator (ESP) in a similar condensation system at around 30 °C. The remaining gases, mainly CO_2, CO, some CH_4 and H_2 as well as vapors of C_2-C_5-alkanes, alkenes and some other volatile organics are actually

flared off, but could be combusted to supply the process energy in commercial applications. Details on the principal design of the pyrolysis plant have been published earlier [13].

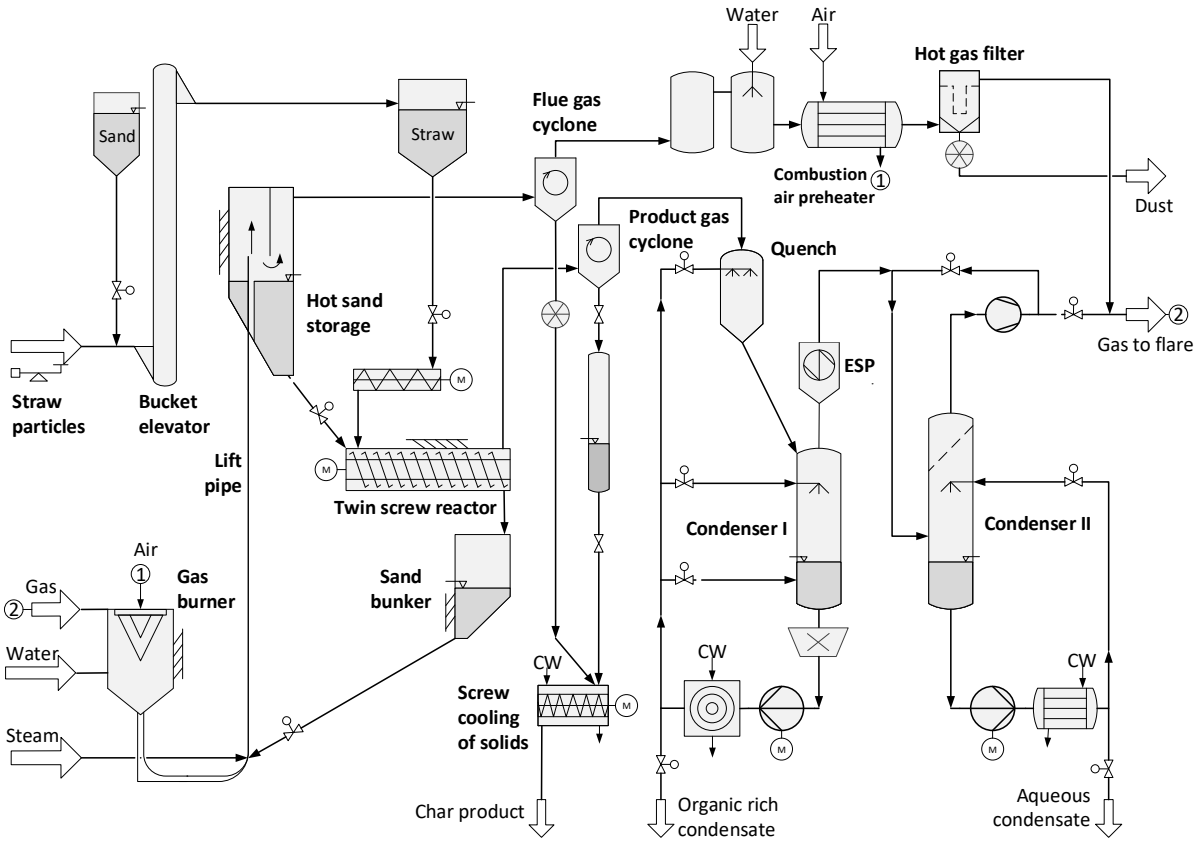

Figure 1: Flow chart of the bioliq® pyrolysis plant.

Experimental test runs at the fast pyrolysis pilot plant are performed in test campaigns with a typical duration of one to two weeks, in which the plant is operated 24/7 in a three or four shift system, respectively. Experimental goals and operation mode have varied throughout the years, but the overarching goal has been a stable and long-term operation with feedstock and the production of pyrolysis products for the use in the subsequent process steps of the bioliq® process. Thus, a typical course of a campaign is as follows: Startup of the plant, which includes the activation of all measuring devices, auxiliary units, heating up the heat carrier system and reactor, starting the condensate circuits etc. This is followed by operation with feedstock under defined

conditions, with as little interruptions as possible. Thereafter shutdown of the plant in a safe state, in which no supervision by personnel is necessary. Shutdown also includes handling of the products, i.e. weighing and transfer steps. Inspection and cleaning of the plant is performed in the follow-up when plant conditions allow for it, e.g. when temperatures are low enough to open apparatuses and piping safely.

2.2 Balancing method for the bioliq® pyrolysis pilot plant

The size, setup and operational concept of the pilot plant results in a more complex balancing method compared to a bench-scale unit. **Figure 2** outlines the plant parts, material streams and measurement points that are relevant for setting up mass balances, which are related to the biomass input and the output of pyrolysis product fractions.

Integral mass balances for the plant are performed for the entire period of a test campaign during the time of feedstock operation. This comprises the time between the first and last feeding to the reactor, including periods of stagnation and standby. Additionally, periods of steady-state biomass operation of several hours are defined and assessed in greater detail. Due to the methods for the determination of input and output streams to/from the plant, mass balances for short periods are less reliable. Fluctuations arise from the uncertainty of the measuring track, the heterogeneity of the feedstock and deviations in the process conditions [15].

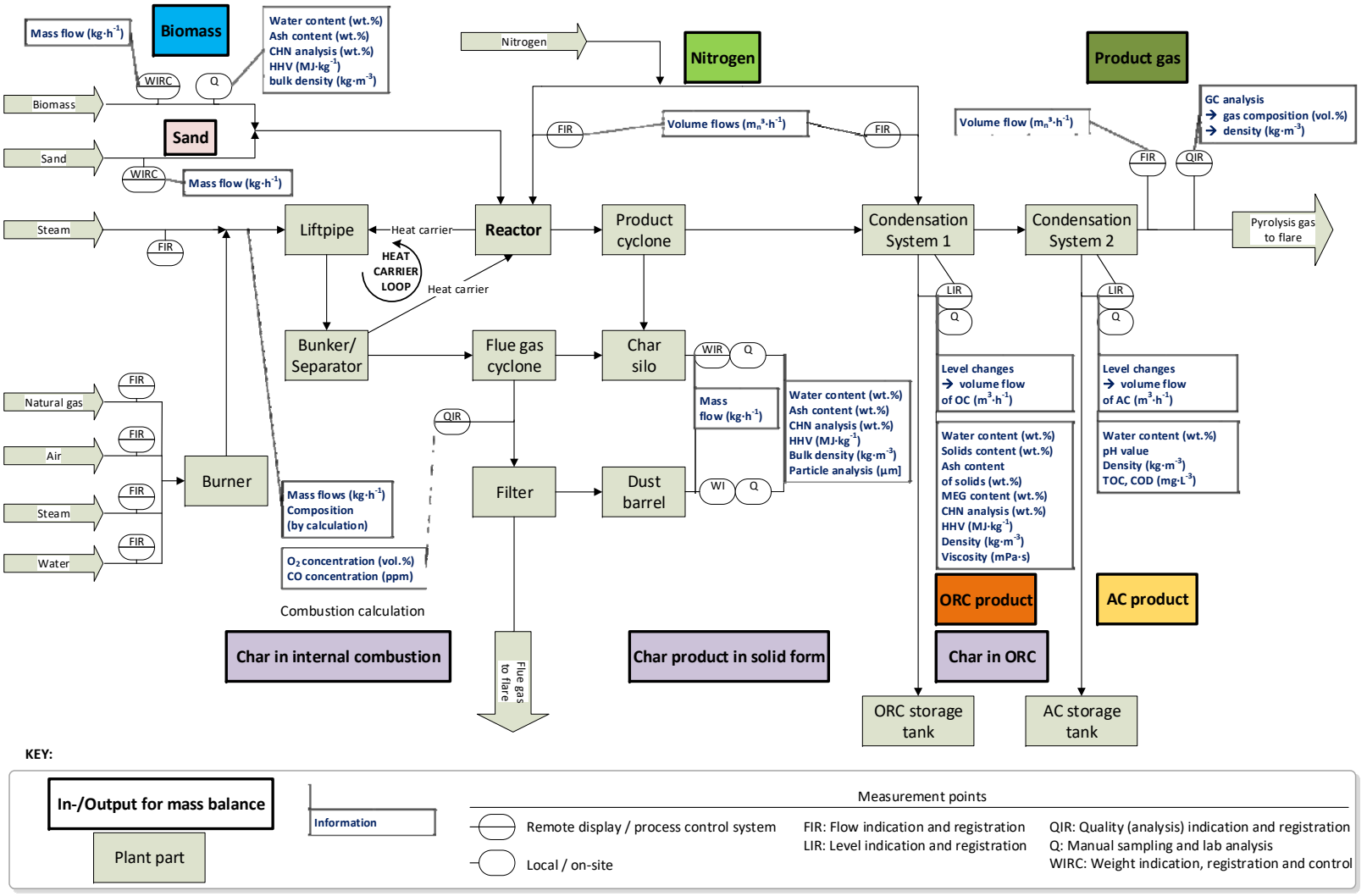

Figure 2: Simplified chart with input and output streams, measurement points and data provided for mass balance determination of the bioliq® pyrolysis plant.

Feed input. The feed input to the reactor is determined on a mass basis using a belt scale. This device is located between the storage bunker for ground biomass and the bucket elevator, which transports the feedstock to a small buffer tank. From there, a screw conveyor transports the feedstock to the reactor. The volumetric dosing via the screw is controlled by the speed of the screw as pressure fluctuations in the reactor may cause instabilities to gravimetric systems at this point. Despite calibrations of speed vs. mass flow for each feedstock prior to operation, a volumetric dosing for inhomogeneous material such as wheat straw is not reliable, as its bulk density and flow behavior may vary significantly. In steady-state biomass operation, the set-point for the mass flow of the belt scale is set to a constant value and the fill level of the buffer tank is kept constant within a defined range by adjusting the speed of the conveyor screw manually. Feedstock samples are taken periodically – typically composite samples for one shift or one day – directly at the belt scale. Their water and ash content are used, inter alia, for calculating balances on moisture- or ash-free basis and to calculate the amount of sand abrasion in the products.

Sand input. During circulation of the heat carrier sand, a certain amount leaves the heat carrier loop due to abrasion and losses to the flue gas and product gas lines. Therefore, fresh sand is fed into the system from a silo via a metering screw with scale when necessary, depending on the fill levels of bunkers for hot sand, which are kept within a certain range during operation. The amount of sand in circulation is not measured directly due to the process conditions (temperatures above 500 °C), but this is not necessary for the mass balance. The amount of sand input is used for cross-check calculation of abrasion.

Input of nitrogen. The flow of nitrogen as inert gas into the reactor and the electrostatic precipitator (ESP) is measured and controlled via flow meters and control valves. The total input

of nitrogen for the integral mass balance is determined by integration of the flow values over the time of production of pyrolysis gas.

Char product. Due to the process design of the bioliq® pyrolysis unit, solids – i.e. char (including ash) and abrasion from the heat carrier loop – are recovered in several forms. The main share, which is recovered by the product gas cyclone and the flue gas cyclone, is conveyed to and stored in a silo. After separation in the flue gas cyclone, the remaining solids in the flue gas are separated in a hot gas filter and stored in steel barrels. A certain amount of solids passes the product gas cyclone and is precipitated with the organic rich condensate (ORC) in the first condensation system. Another share of the solid product is carried over to the heat carrier loop, where it is internally combusted in the so-called lift pipe, providing additional energy for heating the sand. The amount of char product (including ash) is calculated by summing up masses of solids from silo and dust barrels, ORC and internal combustion minus sand abrasion.

The amount of solids recovered in the silo and barrels is determined by weighing, determination of its properties after taking representative samples is done manually. The amount of solids in the ORC is determined by multiplying the amount of ORC with its solids content (for details see section ***"Organic rich condensate and aqueous condensate"***).

The amount of solids for internal combustion is obtained through combustion calculation. Mass flows of the input streams to the gas burner and of the additional fluidization steam upstream of the lift pipe are measured by flow meters, the composition of the flue gas downstream of the lift pipe by online gas analysis. The solids for internal combustion are assumed to consist of pure carbon due to the lack of an exact analysis of their composition. For the calculation of their amount, all periods featuring internal combustion are considered. This comprises periods during which

biomass is fed to the reactor followed by a certain time span of heat carrier circulation, during which the remaining solids are burned, detectable through flue gas analysis.

Organic rich condensate and aqueous condensate. Both organic rich and aqueous condensates are stored in tanks prior to their transfer to the subsequent bioliq® process units. As the tanks are not equipped with load cells and their volume is quite large, the mass amounts are calculated considering level changes in the calibrated buffer vessels of the condensation systems and the density of the media, determined by offline measurements of samples. Measurements of solids content and their respective ash content are used to calculate the yield of solids in the ORC. The water content is used for calculating the total organic liquid yield (OLY), which is the mass of all organic liquid both in ORC and AC divided by the mass of feedstock on a dry basis. Also, the solids content is ORC is excluded (Equation 1).

$$\mathrm{OLY} = \frac{m_{\mathrm{ORC}} - m_{\mathrm{H_2O,ORC}} - m_{\mathrm{Solids,ORC}} + m_{\mathrm{AC}} - m_{\mathrm{H_2O,AC}}}{m_{\mathrm{Biomass,dry}}} \qquad \text{(Equation 1)}$$

The water free organic liquid yield is a common parameter reported in scientific literature, which allows for the comparison with other published results.

Product gas. For the calculation of the product gas, two different methods can be applied. (a) Knowing the nitrogen input to the plant and the concentration of nitrogen in the product gas, measured by an online gas chromatograph (GC), the amount of product gas can be calculated. (b) The product gas flow rate is measured by a gas meter on a volume basis. Nitrogen input to the reactor and the electrostatic precipitator is subtracted. The mass of product gas is calculated considering the gas density determined by the GC. The water content in the product gas is based on the assumption of saturation of steam at a given temperature as water vapor is not analyzed by the GC.

3 Results

3.1 Mass balance results 2015–2018

Over the years, many modifications and optimization steps have been implemented in the plant, see chapter 4 for more details. For reasons of better operational stability leading to more reliable balances, we only report on the results of the last five campaigns (numbers with internal nomenclature: 2015/05-06 to 2018/41-42) with wheat straw here. Results on campaigns prior to that are reported in [12, 13].

For the campaigns 2015/05-06 to 2018/41-42, steady-state periodes were selected during which the main operation parameters remained constant. in. The reactor temperature was 500±0.5 °C, showing very little deviation from the set value of 500 °C. The temperature of the heat carrier upstream of the reactor was 540–565 °C, depending on the temperature in the sand bunker and valve opening positions in the heat carrier loop as well as on the biomass feed rate. Nitrogen inertization to the reactor was controlled in the range of 10–15 Nm^3h^{-1}. The temperature at the bottom of the first condenser varied between 85 and 95 °C, whereas temperature of the second condenser was in the range of 22–34 °C.

As can be seen from **Table 1**, total straw feed (kg) and its average rate for each campaign ($kg \cdot h^{-1}$) differ significantly, which is explained by different goals of the campaigns or problems in the experimental runs. Nevertheless, water and ash content of the feed material during the considered campaigns lie within a relatively narrow range (9.3±0.2 wt.% or 5.7±0.3 wt.%, respectively), so comparability with respect to the feed material is given, even though over the years different batches of wheat straw had to be used due to the huge amounts of material needed and the limitations in stock-keeping and storability. Mass balance closure was between 99 and 104 wt.%.

Determination of product gas yield is assumed to contribute most to the difference in mass balance closure.

Table 1. Overview on mass balances in the campaigns between 2015 and 2018 with wheat straw feed. Mass yields of products are given as mass fraction of biomass input (as-received basis). Organic liquid yield (OLY) is reported on a dry basis for reasons of comparability.

Campaign	Straw	Straw	Straw	Straw	Yield	Yield	Yield	Yield	Yield	Yield	Ratio
Time period	Feed total, ar	Feed rate, ar	Water content	Ash content	Char[a]	ORC	AC	NCG	Sum	OLY	CO/CO_2[b]
	kg	$kg \cdot h^{-1}$	wt.%	wt.%, dry	wt.%	wt.%	wt.%	wt.%	wt.%	wt.%, dry	(-)
2015/05-06	36277	273	9.0	5.2	21.2	36.6	24.7	17.0	99.6	39.0	0.73
2015/46-47	39465	334	9.5	6.1	23.0	33.2	20.8	22.4	99.4	34.0	0.66
2016/29	11533	288	9.3	5.4	24.2	31.0	25.9	20.3	101.4	35.0	0.70
2017/19-20	42520	315	9.5	5.9	24.1	31.1	22.6	25.4	103.2	32.7	0.66
2018/41-42	51122	322	9.4	5.8	24.3	33.6	22.7	19.0	99.5	34.0	0.60
Average			9.3	5.7	23.4	33.1	23.4	20.8		35.0	0.67
Standard deviation			0.2	0.3	1.2	2.1	1.8	2.9		2.2	0.04

[a]: including fraction for internal combustion and solid fraction of ORC; ORC is given here as solids-free

[b]: derived from online gas chromatograph measurements of NCG

ORC: Organic rich condensate; AC: Aqueous condensate; NCG: Non-condensable gases; OLY: Organic liquid yield

The values given in **Table 1** for yield of non-condensable gases (NCG) are calculated with "Method a", using a nitrogen concentration measured by the GC and its mass flow to the reactor and ESP. "Method b" has a high uncertainty as the flow meter in the product gas can be contaminated by constituents of the product stream over time, thus delivering incorrect values. Yet, "Method a" is strongly affected by the quality of GC measurements. Ideally, the measuring

values from GC should be available every 15 min and re-calibration should be performed regularly (at least once a day). In practice, the GC was often not available due to problems with the sampling line (filter, pipes) or measurements were only performed at specifically selected periods of time in order to spare the system from contamination with pyrolysis condensates.

Yields of ORC and AC vary significantly due to different process conditions in the condensation systems. The total organic liquid yield (OLY), however is 32–35 wt.%, with the exception of campaign 2015/05-06 (39 wt.%). The latter stands out with lowest ash content in the biomass, lowest char and NCG yield and highest CO/CO_2 ratio. This result corresponds to observations made previously [11], suggesting that a decrease in ash content leads to an increase of OLY and CO/CO_2 ratio at the expense of char and product gas. However, it is likely that changes in process conditions will contribute to the effects observed. Prior to campaign 2015/05-06, modifications in piping and reactor geometry were implemented (see also **Table 5**). Clean surfaces on piping and especially on the reactor lid might have reduced secondary heterogeneous pyrolysis reactions, thus enhancing OLY and reducing charring reactions (compare [16]). This hypothesis is supported by data from the campaign prior to 2015/05-06, where OLY was only approx. 29 wt.% at a high char yield of approx. 26 wt.%. During the subsequent plant inspection, massive deposits of char were found on the reactor walls.

A more detailed discussion of yields consolidated with a process demonstration unit of the same design can be found in chapter 3.2.

Comparison of integral balances with steady-state period balances. It is desirable to establish balances during an experimental campaign over a certain period of steady state operation to allow for efficient investigation of parameter studies. Also, reducing balances to periods of steady state operation will eliminate artefacts that result from all transient operational conditions,

including startup and shutdown. The required information is available and **Table 2** shows an example of results from the 2017/19-20 campaign.

Table 2: Comparison of online balances from steady-state conditions and the integral balance of the entire campaign 2017/19-20. *I, II, III* represent long periods of several hours, subsets of 1 or 0.5 h within are labeled *a–d*.

Campaign Time period	Duration	Straw Feed rate, ar	Yield Char	Yield ORC	Yield AC	Yield NCG	Yield Sum	 OLY
	h	$kg \cdot h^{-1}$	wt.%	wt.%	wt.%	wt.%	wt.%	wt.%, dry
I	18.0	346	23	30	24	23	100	31
Ia	0.5	349	n/a	37	24	21	n/a	34
Ib	1.0	349	25	23	33	22	104	28
Ic	1.0	291	29	42	25	27	122	42
Id	0.5	300	29	41	25	25	119	41
II	7.0	353	26	34	21	23	104	34
IIa	1.0	356	26	34	24	21	105	34
III	6.0	408	27	26	24	21	98	28
IIIa	1.0	409	24	26	29	20	99	30
Mean long periods			26±2	30±3	23±1	22±1		31±3
Mean short subsets			27±2	34±7	26±3	23±2		35±5
Entire campaign	135	315	24	31	23	22	100	33

Apart from different feed rates, operational parameters were not changed over the course of this campaign. It can be observed that the heterogeneity of balances derived from steady-state operation time periods increases with shorter balancing periods. Also, the mean of these subsets deviates significantly from the integral balance of the entire campaign. This observation is

primarily attributed to the problem of online determination of the biomass feed rate into the reactor. Mass flow is measured with good precision in a conveyor belt at the outlet of the biomass storage. However, after that there is a bucket elevator (i.e. a time lag) to a buffer tank located on top of the reactor. A volumetric screw feeder conveys the feedstock from this buffer tank to the reactor. The filling level of the buffer tank is not precise enough to adequately calibrate the volumetric feeding screw to the mass flow measured at the conveyor belt. Consequently, mass flow determination is very good for the integral campaign and becomes less reliable as the selected balancing period shortens. Another example is that of the high OLY yields in the relatively short steady state periods Ic and Id. The determination of the ORC (and thus OLY) yield is affected by its periodical release from the condensate loop and thus chaning mass flow rates. Also the varying filling level of the buffer-tank may change, which is used for calculation the ORC yield, and thus affect its more precise determination for short periods of time. This adversely affects the mass balance accuracy for steady-state operational time periods, insofar that they cannot be reliably interpreted. Hence, all evaluations from this pilot plant should only be based on integral balances.

3.2 Comparison of process development unit and pilot plant

A process development unit (‘Python’) has been constructed and operated in parallel to the bioliq® fast pyrolysis pilot plant. This smaller unit shares the same basic process concept, including a twin screw mixing reactor with a continuous heat carrier loop. It has a feedstock capacity of around 10 $kg \cdot h^{-1}$ and thus represents a downscale by a factor of 50. Also, reactor geometry between the two units can be considered to be similar according to the rule of partial similarity based on a dimensional analysis [17]. There is a difference in the sequence of biomass and heat carrier inlet: While biomass is inserted first in the Python unit, the bioliq® reactor requires that the heat carrier is inserted first and that the feedstock is then dropped onto the heat carrier. It has been shown that

the latter design approach leads to better initial heat transfer, which dominates the temperature profile up to the reaction temperature [18]. Another potentially important difference is the duration of an experimental campaign: While the bioliq® pilot plant is typically operated for one to two weeks (i.e. up to 250 h operation with feedstock, the longest period reported here was 170 h), the typical runtime of the Python unit is 3-4 hours. The difference in operational time directly affects the aging reactions inside the recirculation loop of the quench system to recover the ORC, which has been shown to occur to a significant extent [13]. A steady-state residence time distribution of the produced ORC is not reached during the short operational time of the Python unit, i.e. it has to be expected that aging reactions will be less compared to the longer runtime of the bioliq® pilot plant. These two differences in design and operation are expected to counteract each other in terms of an assessment of the liquid yield obtained from these two units.

The yields of ORC, AC, char, and gas in the Python unit for the same wheat straw feedstock as used in the bioliq® pilot are 39.7±1.9 wt.%, 11.8±1.8 wt.%, 22.5±0.2 wt.%, and 21.7±2.5 wt.%, respectively (mass-based on feedstock input as received). The organic liquid yield observed in the Python unit is 28.9±2.1 wt.% (based on dry feedstock). The total condensate yield is comparable to that observed in the bioliq® pilot plant within the heterogeneity of the results and comparable to fast pyrolysis of wheat straw reported elsewhere [19]. There is an obvious shift from AC to ORC yield in the Python unit as compared to the bioliq® pilot plant. One likely reason is the increased ethylene glycol content in the ORC produced by the Python, which originates from the non-displaced startup material of the quench system. Ethylene glycol tends to attract water, which in turn is lost for the aqueous condensate yield.

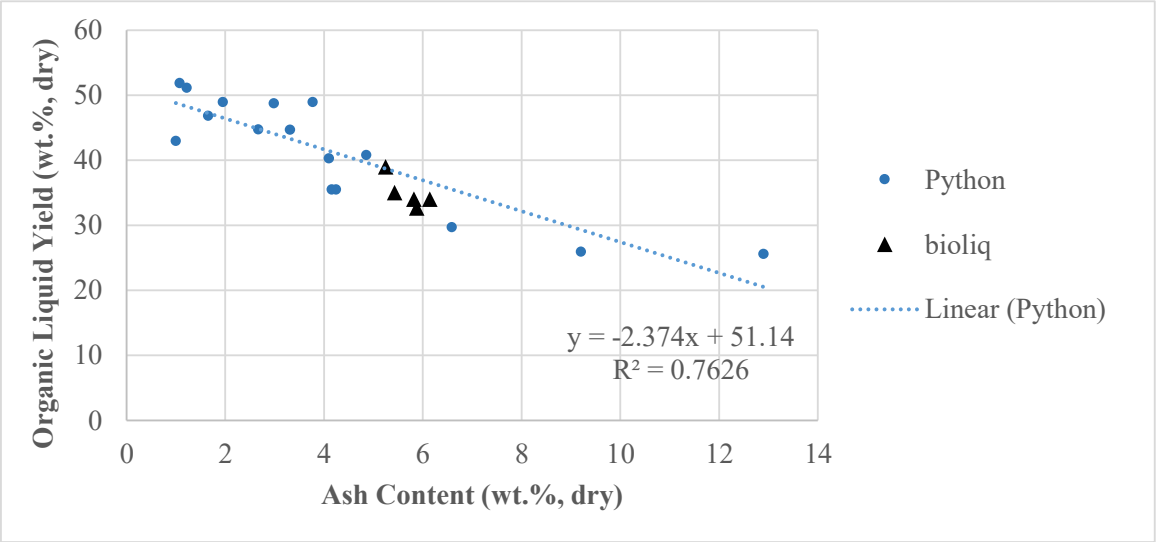

Figure 3. Organic liquid yield from the 'Python' process development unit for a variety of feedstocks and for the 'bioliq®' pilot plant campaigns with wheat straw.

The organic liquid yield (OLY) of both units is comparable to results for wheat straw fast pyrolysis reported elsewhere [20]. The observed difference of 28.9 vs. 35 wt.% in the mean of the two units (compare above given value with **Table 1**) is significant (p=0.006). This difference can be explained by different feedstock preparation/transportation as shown below. The Python process development unit has been operated with a variety of feedstock and results of the total organic liquid yield obtained from these runs are shown in **Figure 3**. These experiments followed the method outlined elsewhere [21]; all data points shown for the Python unit represent mean values from runs executed at least in duplicate. The organic liquid yield is plotted over the ash content of the feedstock and a linear trendline is added, similar to other studies [22, 23]. The data for ash content >8 wt.% indicates that a linear trend is not suitable for the entire range of ash content covered here, which has been reported elsewhere, too [11]. Compared to the other linear trends reported in literature it becomes obvious that the overall organic liquid yield is in the same order of magnitude as reported for other fast pyrolysis test rigs, but slightly less as shown by the

lower y-intercept observed here. The reasons for the comparably lower organic liquid yield observed here are optimization potential for the hot gas residence time [24], aging reactions of the produced oil inside the quench recirculation system, and optimization potential for initial heat transfer as noted above. The organic liquid yield from the bioliq® pilot plant is also plotted in **Figure 3**. There is a significant difference in ash content of the feedstock fed into the reactor even though the same biomass source has been used (Python data points for 6.6 and 9.2 wt.% ash content). It is concluded that ash is selectively removed from the feedstock during feedstock pretreatment in the bioliq® pilot plant, most likely during pneumatic transport into the storage silo, which involves gas/solids separation in a cyclone. Fines, which typically have a high ash content, are carried over with conveying air flow and removed by a subsequent filter instead. It is concluded that the organic liquid yield of both units is indeed comparable and that the observed difference is primarily caused by the difference in ash content of the feedstock inserted into the pyrolysis reactor.

3.3 Product characteristics

Description of laboratory characterization methods and results for previous campaigns were reported in detail in [12, 13]. Methods have not changed since then.

Table 3 shows values of properties that are of relevance for plant operation and further utilization for ORC (including solids), AC and solid char product (recovered in the silo) for the last five campaigns (2015/05-06 to 2018/41-42). Water content in ORC was adjusted for a flowable and homogeneous product by controlling condensation temperature in the range of 85–95 °C and was around 13–16 wt.% on average for the samples considered. Solids content of ORC varied in a broad range (6–16 wt.% on average), which is not directly adjustable by process control but an effect of growing deposits in the section of the product gas cyclone. For a subsequent use in bioliq®

gasification, these high loads of solids with high ash-content are basically no problem, however, viscosity increases considerably, which creates problems in storage, pumpability and atomization during spraying. For the 2018/41-42 campaign, viscosity measured at 80 °C showed maximum values of up to 600 mPa·s, which led to a temporary failure of the circulation pump in the condensation circuit. Viscosity was then lowered by controlled, occasional addition of with MEG (monoethylene glycol) for dilution, which is also used as startup inventory for the condensation circuit due to its good miscibility, flowability and high vapor pressure. The homogeneity and phase stability of fresh bio-oil samples in the 5 campaigns considered was satisfying for the most part, except for campaign 2018/41-42 and samples with a water content of around 20 wt.% or higher. This issue is known and typical for FPBOs from ash-rich feedstock [23, 25]. A comprehensive review on the issue of bio-oil multiphase behavior and phase stability of bio-oils was compiled by Oasmaa et al. [26].

Properties of AC gained at a condenser temperature in the range of 22–34 °C were relatively constant for all campaigns, with an average water content of 81–83 wt.% and a pH value between 2.5 and 3.0. The particle content could not be quantified with our methods but is negligibly low due to the well-functioning electrostatic precipitator upstream of the AC condensation circuit. Average mineral content of solid char product is 27–30 wt.%. The high ash content is explained by a significant accumulation of minerals from feed material in the char during fast pyrolysis. In the campaigns, the accumulation factor of wheat straw (ash content 5.1–6.1 wt.% on a dry basis) to char was in the range of 4.6–5.5. In experiments with wheat straw in the Python unit with a higher ash content in the biomass (8.0 wt.%), the accumulation factor was only 3.6 on average, but the mineral content of char (32 wt.%) was in the same range as above [27].

Table 3. Properties of products as received during the campaigns between 2015 and 2018. Values reflect the mean values and their standard deviation of samples taken periodically during operation.

Property	Dimension	2015/05-06	2015/46-47	2016/29	2017/19-20	2018/41-42
				Organic rich condensate (ORC)		
Water content	wt.%	14 ± 4	16 ± 5	13 ± 5	14 ± 4	16 ± 4
Solids content	wt.%	8 ± 2	6 ± 2	8 ± 2	9 ± 4	16 ± 4
Inorganic material	wt.%	1.0 ± 0.4	0.7 ± 0.2	1.2 ± 0.3	1.2 ± 0.4	2.9 ± 0.4
Density (20 °C)	$kg \cdot m^{-3}$	no data	1180 ± 20	1200 ± 20	1195 ± 9	1190 ± 10
Viscosity (80 °C)	mPa·s	40–80	20–90	20–120	25–190	200–600 (!)
Homogeneity		mainly homogeneous	mainly homogeneous	mainly homogeneous	mainly homogeneous	partly inhomogeneous
HHV	$MJ\ kg^{-1}$	23 ± 1	23 ± 2	23 ± 1	23.6 ± 0.8	22.9 ± 0.7
C	wt.%	55 ± 3	53 ± 4	54 ± 2	55 ± 1	54 ± 2
H	wt.%	7.5 ± 0.3	7.3 ± 0.3	7.3 ± 0.2	7.3 ± 0.1	7.1 ± 0.1
N	wt.%	1.2 ± 0.1	<0.5	0.7 ± 0.1	1.0 ± 0.1	0.9 ± 0.1
				Aqueous condensate (AC)		
Water content	wt.%	81 ± 2	81 ± 1	83 ± 2	82 ± 2	81 ± 2
pH value (20 °C)	-	2.8 ± 0.4	2.5 ± 0.1	2.6 ± 0.1	2.9 ± 0.1	2.8 ± 0.1
Density (20 °C)	$kg \cdot m^{-3}$	1018 ± 1	1018 ± 4	1014 ± 2	1012 ± 1	1013 ± 3
HHV[a]	$MJ \cdot kg^{-1}$	4.1 ± 0.1	4.2 ± 0.3	4.0 ± 0.4	4.1 ± 0.1	4.1 ± 0.3
TOC	$mg \cdot L^{-1}$	96000 ± 5000	94000 ± 3000	82000 ± 7000	87000 ± 3000	90000 ± 5000
COD	$mg \cdot L^{-1}$	287000 ± 9000	296000 ± 30000	280000 ± 30000	287000 ± 9000	280000 ± 20000
				Solid char product		
Mineral content	wt.%	28 ± 6	29 ± 2	30 ± 2	27 ± 2	29 ± 2
Particle size d95[b]	µm	74 ± 3	69 ± 5	93 ± 11	89 ± 3	83 ± 8
HHV	$MJ \cdot kg^{-1}$	23 ± 1	22 ± 1	22 ± 1	23 ± 1	22 ± 1
C	wt.%	60 ± 2	58 ± 2	57 ± 2	60 ± 3	58 ± 2
H	wt.%	2.4 ± 0.1	2.7 ± 0.1	2.1 ± 0.1	2.5 ± 0.1	2.2 ± 0.1
N	wt.%	0.9 ± 0.1	0.8 ± 0.1	0.8 ± 0.1	<1.0	0.9 ± 0.1

HHV: Higher heating value; TOC: Total organic carbon; COD: Chemical oxygen demand.
[a]: calculated, not measured; [b]: Waddel disk diameter; 95 % of all particles ≤ d95

Indicated particle sizes (*Waddel disk d95*) are below 100 µm for all campaigns, showing deviations which may arise from differences in separation performance of the product gas cyclone and variations in biomass particle sizes. Particle size characterization for wheat straw char particles is complex due to their non-spherical shape and is discussed in greater detail elsewhere [28].
Dry composition, gas density and higher heating value of pyrolysis gas during steady state biomass operation are listed in

Table 4. The nitrogen content varies significantly due to differences in nitrogen feed for inertization of reactor and electrostatic precipitator in the different campaigns. However, after subtraction of nitrogen from the gas (theoretical calculation), on a nitrogen-free basis the concentrations of the remaining gas components show only minor deviations for the campaigns considered (e.g. 50.2–53.4 vol.% for CO, 31.9–36.5 vol.% for CO_2). The ratio of CO/CO_2 has already been discussed in chapter ***"3.1 Mass balance results 2015–2018"***. It should be noted that oxygen in the product gas is an indicator of leakage. Its concentration is usually below 0.3 vol.%, but in campaign 2018/41-42 it reached values of up to 1.0 vol.%, probably caused by infiltration in the 'cold' section downstream of the quench cooler.

3.4 Product utilization

Details on preparation, characteristics, handling and product utilization strategy have been previously discussed in detail [29, 30]. While the char-containing, straw-based ORC with a higher heating value of > 20 $MJ \cdot kg^{-1}$and a solids content of approximately 5–15 wt.% can be used directly in the subsequent gasification process, suspensions consisting of AC (HHV approx. 4 $MJ \cdot kg^{-1}$), and straw char (calorific value approx. 22 $MJ \cdot kg^{-1}$) still qualify as fuel for the gasifier. Henrich et al. calculated that an efficient use of the combustion energy of the pyrolysis gases is

sufficient for a self-sustained fast pyrolysis process [31]. This is discussed in more detail below. Pyrolysis gas is not used within the demonstration plant but is burnt off in a flare. In a future installation it may be used for supply of heat energy to the reactor and for biomass pre-drying.

Table 4. Composition and derived properties of pyrolysis gas during the campaigns between 2015 and 2018. All values on dry basis as measured by online-GC. Values reflect the mean values and their standard deviation of measurements during steady-state operation.

Gas component	Dimension	2015/05-06	2015/46-47	2016/29	2017/19-20	2018/41-42
N_2	vol.%	46.6 ± 0.9	37.9 ± 0.6	33.3 ± 4.1	36.1 ± 2.7	39.6 ± 1.4
CO_2	vol.%	26.8 ± 0.6	32.2 ± 0.4	34.0 ± 2.2	33.3 ± 1.6	32.3 ± 1.3
CO	vol.%	19.5 ± 0.5	21.2 ± 0.2	23.7 ± 1.4	21.9 ± 0.7	19.3 ± 0.6
CH_4	vol.%	3.3 ± 0.1	4.0 ± 0.1	4.1 ± 0.3	3.9 ± 0.2	3.7 ± 0.2
H_2	vol.%	1.0 ± 0.1	1.3 ± 0.1	1.4 ± 0.1	1.3 ± 0.1	1.2 ± 0.1
C_2H_6	vol.%	0.4 ± 0.1	0.6 ± 0.1	0.6 ± 0.1	0.5 ± 0.1	0.5 ± 0.1
C_3H_8	vol.%	0.5 ± 0.1	0.5 ± 0.1	0.5 ± 0.1	0.5 ± 0.1	0.5 ± 0.1
C_4's	vol.%	0.7 ± 0.1	0.8 ± 0.1	0.9 ± 0.1	0.8 ± 0.1	1.0 ± 0.1
C_5+	vol.%	1.1 ± 0.1	1.3 ± 0.1	1.4 ± 0.1	1.4 ± 0.1	1.3 ± 0.1
O_2	vol.%	0.14 ± 0.09	0.16 ± 0.03	0.14 ± 0.10	0.18 ± 0.07	0.70 ± 0.27
Normal density[a]	$kg \cdot m_n^{-3}$	1.45 ± 0.02	1.48 ± 0.01	1.50 ± 0.07	1.49 ± 0.05	1.49 ± 0.03
HHV, mf without N_2[a]	$MJ \cdot kg^{-1}$	8.4	8.4	8.4	8.3	8.3

[a]: calculated, not measured

3.5 Process heat supply

Process heat is required to operate fast pyrolysis units since the reaction in them is endothermic. Additional auxiliary energy may be required to operate a fast pyrolysis plant depending on its design. In most industrial-scale fast pyrolysis plants, heat is supplied by combusting the byproducts char and pyrolysis gas. The latter contains a significant amount of >C2 organics, which are made

up by aerosols in case of incomplete removal and vapors (that form the aqueous condensate in the bioliq® unit), because the final condensation temperature is typically >50 °C. The high final condensation temperature avoids dealing with an aqueous condensate fraction while controlling the water content of the produced FPBO. Excess heat is generated by combusting the byproducts and most units are integrated into a combined heat and power system to sell electricity and steam.

The bioliq® concept aims at optimizing carbon efficiency across the entire valorization chain from biomass residues to 2nd generation fuels. Downstream use of the carbon-rich char byproduct is desirable to enhance carbon efficiency. A second aim is to offer a solution for the conversion of biomass residues with high ash content. The importance of the char byproduct increases in this case, not only due to the fixation of the inorganic compounds, but also due to an increased carbon recovery via the char [32]. If the char is recovered for downstream use, the heat supply to the process becomes an interesting aspect, irrespective the consideration of a second condensation stage to recover aqueous condensate.

The existing bioliq® pilot plant is a research facility and not energetically optimized. One important implementation to reduce operational complexity is to flare the produced pyrolysis gas. All auxiliary heat required to run the process is supplied by natural gas, either directly in a combustion chamber or indirectly via steam from a natural gas fired boiler. The online measurements available can be used to assess how much of the natural gas can potentially be replaced by pyrolysis gas. This has been done for time periods of steady state operation even though they are less reliable than the integral balance. It was decided to do so due to the high heat requirement to warm up the unit and the heat carrier inventory to process temperature, which will significantly impact the result of such an assessment. From the natural gas supplied during steady state operation (excluding the natural gas required to sustain the flaring of pyrolysis gas), a mean

value of 93±17 % can be potentially replaced by the pyrolysis gas. This value is very heterogeneous because it directly relies on the measurement of pyrolysis gas flow, which proved to be problematic.

As noted above, there is room for improvement from an energetic point of view. About a third of the steam consumed by the process is used in the heat carrier lift pipe as additional lift gas, another third is added to the combustion chamber, and the last third is used as a quenching medium for the flue gas leaving the heat carrier loop to avoid excessive heat in the filter system. With an optimized heat recovery system, this latter third can surely be saved. Also, it is to be expected that combustion of pyrolysis gas will lead to a larger volume flow compared to natural gas with the same heat load, which will further reduce the additional lift gas requirements supplied by the steam. A theoretic assessment of an optimized case with heat recovery alternatives based on the bioliq® fast pyrolysis plant shows that potentially even excess heat can be made available, e.g. to dry the incoming feedstock [24].

4 Experience with design and operation mode

As the scope of this paper is limited to the experiments with feedstock wheat straw, we show the development from the first tests with wheat straw in 2009 up to the campaign in 2018, which was the last with this feedstock for the time being. Since 2019, alternative feedstocks such as miscanthus have been investigated.

4.1 Chronology of test campaigns with wheat straw

After mechanical completion of the plant in 2008 and startup tests, the first test campaign with wheat straw was conducted in 2009. As can be seen in **Table 5**, the amounts of pyrolyzed straw during the first 7 campaigns up to 2011/14 are rather modest (10.4 t in total). The elimination of plant design deficiencies was time-consuming due to long delivery times of equipment and spare parts, among other things. Major modifications in design, apparatuses, piping, equipment, instrumentation, control, automation, process control system and operation mode were implemented. This period can be considered as function testing of equipment and basic training of the technical staff at the plant. From campaign 8 onwards, experimental operation became more reliable. Yet, frequent interruptions and failures prevented steady-state conditions. During campaigns 8–13, long stable periods of wheat straw feeding to the reactor over several hours were the exception. The replacement of the tube bundle heat exchangers with spiral heat exchangers for the ORC circuit in 2013 and changed process parameters led to a much more reliable operation of the ORC circuit from campaign 14 onwards. Being one of the main issues, this modification had a significant impact and enabled uninterrupted steady-state operation with constant biomass feed for several hours. During long-term operation, new issues such as blocking of product leading piping by deposits and fouling were revealed. Several measures such as acoustic cleaning devices, an automated cleaning unit and modifications of design and geometries of product-carrying parts have been successfully implemented, explained in more detail elsewhere [33]. The stability and duration of steady-state biomass operation periods have been enhanced and representative products for further utilization in the bioliq® process or research projects could be provided. In total, more than 260 tons of wheat straw had been converted by 2018.

Table 5: Overview of campaigns with wheat straw feed after commissioning and of major modifications of the plant. Masses of straw indicate the total amount that was fed during the campaign.

	Campaign	Mass of straw	Modifications implemented in revision prior to campaign
No.	Year/CW	t	
1	2009/14	0.9	"major revision"
2	2010/08	0.6	- Discharge of char (product and flue gas): Installation/modification of various valves in piping for solids - Condensation circuits (ORC and AC) thoroughly modified - ESP installed - Revision of PCS/ICA
3	2010/26-27	0.0	- ESP modified (insulator and inert gas flushing) - Poking devices in vessels for solid product - Various changes in ORC circuit (change of piping and operation mode of heat exchangers)
4	2010/36	1.3	- Heat carrier system: Fluidization optimized (steam inlet), valves modified - Repair of pump for ORC (bearings, sealings, shaft)
5	2010/47	3.4	- ESP modified (insulator and inert gas flushing) - Revision of PCS/ICA - Function tests of ORC and AC circuits, valves - Leak testing
6	2011/12	1.0	- Discharge of char from product gas cyclone optimized - Nozzle diameter in quench system widened
7	2011/14	3.2	Resumption of campaign No.6
8	2011/29	11.5	- Gas measurements: Process gas chromatograph installed - Oxygen measurement for ESP and flue gas analyzer modified - Changes in sand bunker (classification of particles, new sealings…) - Nozzle type quench changed - Revision of PCS/ICA
9	2011/48	12.0	- Macerator prior to pump installed in ORC - Upgrade of various control valves - Revision of PCS/ICA
10	2012/26	0.8	- Cleaning unit quench: Old manual system replaced by automated system - Feed inlet reactor: Pipe shortened; poking unit (+camera) installed - Additional sensors (temperature, pressure) installed
11	2012/28	4.5	Resumption of campaign No.10
12	2012/46	4.4	- Secondary cooling circuit for ORC installed; cooling temperature elevated - Cleaning unit quench further optimized (bearings, lubrication) - Heat carrier loop: Nitrogen pressure ‘cannon’ installed - Nitrogen flushing and poking devices in char collection system (vessels and pipes) optimized
13	2013/20	7.3	- Cleaning unit quench further optimized (extra cooling system) - Buffer tanks for ORC and AC installed (3.5 m³ each)

14	2013/49	14.9	- Change of heat exchangers in ORC circuit: Spiral type instead of tube bundle - Slurry mixing station installed - Char separation enhanced (distance from cyclone to vessel extended, different valve type)
15	2014/19-20	17.6	- Modification of sampling point for product char - Various minor repairs/modifications
16	2015/05-06	36.3	- Quench inlet modified (pipe shortened, auxiliary heating discontinued) - Modification of piping between reactor and quench - Quench nozzles changed (spiral to flat spray type) - Unnecessary 'dead-zones' on reactor lid eliminated, reactor thoroughly cleaned - Various repairs (level sensor flue gas cyclone, trace heaters, pipes) - Flue gas filter: New type installed (ceramic filter candles instead of filter bags) - New instrument for gas flow measurement (range enhanced) - Feeding screw for feed changed (to helical spiral type)
17	2015/46-47	39.5	- 3 new mechanical poking positions in product lines (2x reactor-cyclone; 1 quench-cyclone) - Pipe diameter for biomass feed to reactor enlarged - Product line from reactor to cyclone polished
18	2016/29	11.5	- Acoustic cleaning unit for pipe from reactor to cyclone installed - Optimization of automated cleaning unit (purging station for rod) - Measurement systems for flue gas (humidity and particle content) installed
19	2017/19-20	42.5	Several repairs/maintenance, e.g.: - Product gas blower reconditioned (new cooling system) - Valve type near flue gas filter changed
20	2018/41-42	51.1	- Biomass buffer tank modified; new level sensor; new stirrer - Acoustic cleaning system for pipe quench-cyclone installed; partially automated - Online measurement device (mass flow, viscosity, density) installed in ORC circuit - Biomass preparation: optimization of speed; less blockage

ORC: Organic rich condensate; AC: Aqueous condensate; ESP: Electrostatic Precipitator;
PCS: Process control system; ICA: Instrumentation, control, automation

4.2 Special aspects and challenges during long-term operation

Feed input section. Continuous feeding of straw particles into the reactor is a challenge due to the flow properties of this relatively inhomogeneous material. The chopped straw used in the experiments has a low bulk density, broad particle size distribution, unfavorable fibrous particle shape and the ability to absorb moisture. Bridging and undesirable flow were frequently observed in the feeding section, causing blockages or fluctuations in the material flow. During transport from the cutting section of the plant to the reactor, the material passes two cyclones, a feedstock

storage silo, screw conveyors, a belt conveyor scale, a bucket conveyor, the buffer tank and the metering screw.

The feedstock storage silo with its large volume of 60 m³ is a source of several problems due to its design (size, geometry, outdoor installation, air atmosphere). Depending on ambient conditions – particularly the dew point of ambient air – and residence time, straw particles absorb moisture, which promotes adhesion and agglomeration of particles. Compression of the voluminous material due to pressure from the overlying material may lead to hard clusters, especially on the silo wall. In combination with the observed funnel flow, material on the silo wall can adhere and mold if not removed mechanically during downtime. The above described clusters or carryovers from the wall were found to be hard enough to sustain the subsequent transport up to the reactor, potentially causing blockages in the outlet of the buffer tank and metering screw. Over the last years, the level of straw in the storage silo was held at a relatively low fill level (20–30 %) to provide a sufficient supply for several hours of operation while also reducing mechanical pressure on the bulk. Consequently, the milling section was run with less standby-time to ensure continuous operation. Furthermore, a standard procedure for inspection and removal of residual material from the silo after each test campaign was introduced.

The buffer tank was prone to bridging in the lower conical part and the junction to the feeding screw, being one of the main causes of process interruptions in the past. Potential causes were successfully eliminated in 2017, also leading to change of stirrer and replacement of the level sensor (vibrating level switch) with a non-contact measuring device (radar). With regard to the section of the feeding screw it is worth mentioning that an open helical spiral type showed good results and led to less problems caused by compaction of material than a blade screw with center rod. Nitrogen purging in the direction of biomass flow to the reactor in combination with

temperature monitoring in the feeding screw is of great importance in order to avoid clogging caused by influx of hot pyrolysis vapors into this section. The use of a camera did not work out well as it was susceptible to staining by straw dust and vapors. The inlet to the reactor was also retrofitted due to plugging and now has a shorter but wider inlet pipe that is provided with a poking device.

Deposits in the product gas section. The product mixture released by fast pyrolysis of wheat straw in the twin-screw reactor at 500 °C consists of fine solids (char, ash, abrasion of heat carrier), organic vapors, water vapor and permanent gases. At elevated temperatures, its components interact chemically and physically in complex mechanisms, and components may change their aggregation state during cooling. Porous wheat straw char can absorb condensed high molecular weight components ('tar') that stick to surfaces and build up layers, which harden during evaporation and decomposition at elevated temperatures.

Deposits in pipelines carrying product gas are a challenge in long-term operation as they lead to side-reactions, affect flow dynamics, create undesired pressure loss or even blockages [33]. Deposits were observed throughout the equipment and piping from the twin-screw reactor up to the flare, but particularly in the hot section up to the product gas quench. Preventive measures such as optimization of pipe routing and cross-sections, surface treatment and product path heating reduced clogging to a certain extent, but needed to be supplemented by devices that actively remove growing layers in-situ, i.e. during operation at process temperatures of up to 550 °C. Thermal cleaning by means of periodically controlled supply of oxygen or air is not an option for the plant due to material constraints and the associated safety issues. Different cleaning devices were tested, from manually inserting simple poking rods, through rods equipped with scrubbers to an acoustic cleaning system (provided by company A.W. Akustik). The latter proved to be

favorable for several reasons: (a) comfortable handling and simple automation, reduction of work load for the staff; (b) no mechanically moving parts, thus no risk of jamming; (c) can be used during feed operation; (d) intensity can be controlled as needed. However, the acoustic system induces pressure fluctuations that disturb the usual flow profile of product gas and may release and spread flakes or lumps of hard material to other pipe sections or equipment.

As described before, inspections during campaigns are not performed because of the long cool-down times of equipment. Therefore, no measurements of layer thicknesses are available to quantify the usefulness of the described actions. Conclusions on cleaning actions are drawn from the monitoring of pressure differences across plant sections before and after cleaning.

Product gas cyclone. Deposits in this section have a negative effect on the separation efficiency of solids, which directly affects the yield products and their properties. It has been frequently observed that with increasing duration of pyrolysis operation during a campaign, the solids content in the ORC increased and stagnated at a high level of 10 wt.% and more (extreme case in 2018 up to 20 wt.%), probably due to a disturbed flow profile caused by gradual fouling. Rigorous cleaning of this section after each campaign is of great importance as a preventive measure, but difficult to carry out due to the layout of the plant. The necessary retrofitting has not yet been realized for cost reasons. Currently, cheaper, but time-consuming disassembly (insulation, trace heating, flanges, piping, etc.) is part of the follow-up work of a campaign.

Product quench and condensation loop for organic rich condensate. The quench design installed at the plant is a kind of spray column, where hot pyrolysis gas with an inlet temperature of about 500 °C is mixed with recirculated bio-oil of 80–100 °C. The inlet section of pyrolysis gas at the top of the quench is particularly prone to deposition, which reduces the free cross-section and causes critical pressure losses. Some reduction of deposits was achieved by changing the spray

pattern by re-positioning and changing the nozzle type, and slight modifications in the geometry of the inlet section. The cleaning device used is an in-house development that has been frequently upgraded, as can be seen in **Table 5**. It currently consists of an automated system in which linear and rotary actuators and motors periodically move a rod with specially designed chains in and out of the quench inlet. A cleaning system for the rod including rinsing with tempered solvent was necessary to counteract deposits there, see [33] for more details.

The installation of a macerator in the ORC circuit was a consequence of the experience made with plugging of the quench nozzles, problems with the pump and settling/sedimentation in the piping system. It de-agglomerates and homogenizes the ORC and the suspended solids, and reliably mills even hard deposits originating from the cleaning actions described above.

Controlling the condensation temperature in the ORC circuit is of great importance for long-term operability as well as for product quality. Temperature directly affects the water content in the ORC, which in turn affects the viscosity and phase stability. Fouling on heat exchanger surfaces must be avoided or restricted to an acceptable level during the entire operating time in order to maintain the desired condensation temperature. In the bioliq® plant, the use of two spiral heat exchangers (company: Alfa Laval AB) connected in series in combination with a lower temperature difference between cooling medium and ORC, achieved through the installation of a secondary cooling circuit, worked reliably from its implementation in 2013. The risk of precipitation of viscous organic components with a high boiling point on the boundary layer is reduced by highly turbulent flow in the channels of the heat exchangers and an inlet temperature of the cooling medium of approx. 40–50 °C.

Electrostatic precipitator. The separation of aerosols downstream of the ORC circuit with an electrostatic precipitator works well and prevents carry-over of water-insoluble substances to the

subsequent AC circuit. It should be noted that this is a relatively complex design, with several auxiliary heating circuits, multi-piece insulator and nitrogen purge. For reasons of explosion protection, it is supplemented by a measuring system for continuous monitoring of the oxygen content. This system again consists of various devices (such as cooling systems, a small ESP, pumps, filters, valves, flow meters, blower, etc.) in order to protect the measuring cell from contaminations. Deposits on insulator surfaces of the ESP due to an inappropriate mode of operation can become critical and lead to downtime. Suitably controlling the entire system needs regular maintenance and qualified personnel for the correct adjustment of process values.

5 Further activities

5.1 Improvement of steady state balances

Many of the challenges associated with establishing meaningful mass balances have been solved during the process of constructing, operating, and developing the fast pyrolysis bioliq® pilot plant. This primarily includes online measurement systems for the difficult matrix of most pyrolysis products and their calibration with recognized offline analytics. In a study based on the Monte Carlo method [15], it was found that density measurements of the liquid products is the second main influencing uncertainty towards liquid yield reproducibility. It does not come as a surprise that biomass input characterization is dominating mass balances. This includes mass flow, but also ash and moisture content to better describe the variability of the resulting liquid yields. Wheat straw mass flow is measured with very good precision on a conveyor belt scale, which enables a reliable quantification of the entire feedstock added during a campaign and also for most industrial applications. However, determining mass flow over smaller time scales such as 1 hour becomes more difficult. In such cases, variations in the intermediate feedstock buffer tank placed on top of the reactor (i.e. downstream of the belt conveyor scale) become significant. Experience with wheat

straw in both the bioliq® pilot plant and Python process development unit shows that steady state dosing with a volumetric screw feeder cannot be assumed. Mass balances over 1 hour are also prone to fluctuation based on the heterogeneity of the feedstock composition, primarily its ash content (more precisely its alkali metal). Even though samples have been taken and analyzed regularly, the issue of time-resolved investigation could not be solved within the bioliq® project and requires additional work.

5.2 Process modeling

Modelling of (fast) pyrolysis processes remains a challenge. There is no physically consistent approach that enables representation of feedstock, reaction, and condensation, especially considering the large amount of unknown, high molecular weight components that are typically found in FPBO. It is possible to include one of the existing reaction models for pyrolysis into flowsheet models, but many approaches are still based on describing reaction products based on mass balances from individual experiments, i.e. setting up a descriptive process model. This has also been done for the bioliq® process [34]. These models are still suitable for the investigation of energetic optimization potential. In order to increase conclusions drawn from such studies, more detailed models for the heat carrier loop and pyrolysis gas combustion need to be included. Another issue in improving models for energetic evaluation of the process are condensation models, especially to better describe light volatiles that could potentially be diverted to the gaseous product stream (and in turn be combusted to yield more heat) instead of being recovered with the AC. While modelling of vapor liquid equilibria of FPBO is not straightforward and an ideal behavior of the water as main component cannot be assumed [35], including feasible models for the aqueous fractions appears to be a reasonable next step.

6 Conclusion

With respect to expected yields of the pyrolysis pilot plant, the use of integral balances over the time of an entire campaign is advisable for the setup of bioliq®, as evaluation of selected periods of steady-state operation was observed to be less accurate. Furthermore, comparability of the generated data for different test campaigns must always be regarded critically, considering technical modifications and/or changes in operational mode. Still, the organic liquid yield of the bioliq® pyrolysis plant is in good agreement to a process development plant of the same design and to results for wheat straw fast pyrolysis reported in literature.

Since the first test campaign with wheat straw at the bioliq® pyrolysis plant in 2009, major modifications in hardware and operational mode, such as secondary cooling circuit for ORC and cleaning devices in the product gas section, were successfully realized over the past decade, allowing for stable operation over several days and yielding representative, stable products for further use in the bioliq® process or other research projects.

AUTHOR INFORMATION

Corresponding Author

*E-mail: andreas.niebel@kit.edu

Author Contributions

The manuscript was written with text contributions by all authors. All authors have approved the final version of the manuscript.

Notes

The authors declare no competing financial interest.

ACKNOWLEDGMENT

Pilot plant operation and related R&D investigations are team work. The pilot plant operational team, the analytical team as well as the supporting R&D groups are gratefully acknowledged. Financial support has been provided by the Federal Ministry of Food and Agriculture for the erection of the bioliq® fast pyrolysis pilot plant. The industrial partners, Air Liquide, Bauer MAT and Calida Cleantec is thanked for the fruitful and intensive cooperation.

REFERENCES

1. Scarlat, N., et al., *Integrated and spatially explicit assessment of sustainable crop residues potential in Europe.* Biomass & Bioenergy, 2019. **122**: p. 257-269.
2. Henrich, E., et al., *The Role of Biomass in a Future World without Fossil Fuels.* Chemie Ingenieur Technik, 2015. **87**(12): p. 1667-1685.
3. Venderbosch, R.H. and W. Prins, *Fast pyrolysis technology development.* Biofuels Bioproducts & Biorefining-Biofpr, 2010. **4**(2): p. 178-208.
4. Meier, D., et al., *State-of-the-art of fast pyrolysis in IEA bioenergy member countries.* Renewable & Sustainable Energy Reviews, 2013. **20**: p. 619-641.
5. Oasmaa, A., et al., *Historical Review on VTT Fast Pyrolysis Bio-oil Production and Upgrading.* Energy & Fuels, 2021. **35**(7): p. 5683-5695.
6. Krutof, A. and K. Hawboldt, *Blends of pyrolysis oil, petroleum, and other bio-based fuels: A review.* Renewable & Sustainable Energy Reviews, 2016. **59**: p. 406-419.
7. Xiu, S.N. and A. Shahbazi, *Bio-oil production and upgrading research: A review.* Renewable & Sustainable Energy Reviews, 2012. **16**(7): p. 4406-4414.
8. Venderbosch, R.H., et al., *Stabilization of biomass-derived pyrolysis oils.* Journal of Chemical Technology and Biotechnology, 2010. **85**(5): p. 674-686.
9. Schmitt, C.C., et al., *From agriculture residue to upgraded product: The thermochemical conversion of sugarcane bagasse for fuel and chemical products.* Fuel Processing Technology, 2020. **197**.
10. Dahmen, N., et al., *The bioliq process for producing synthetic transportation fuels.* WIREs Energy and Environment, 2017. **6**(3): p. e236.
11. Troger, N., D. Richter, and R. Stahl, *Effect of feedstock composition on product yields and energy recovery rates of fast pyrolysis products from different straw types.* Journal of Analytical and Applied Pyrolysis, 2013. **100**: p. 158-165.
12. Pfitzer, C., et al. *First results of the bioliq fast pyrolysis pilot plant.* in *Proceedings of the 22nd European Biomass Conference and Exhibition*. 2014. Hamburg, Germany.
13. Pfitzer, C., et al., *Fast Pyrolysis of Wheat Straw in the Bioliq Pilot Plant.* Energy & Fuels, 2016. **30**(10): p. 8047-8054.
14. Dahmen, N., et al. *bioliq®-pilot plant for the preparation of synthetic fuels - operating experience*. in *Proceedings of the 27th European Biomass Conference and Exhibition*. 2019. Lisbon, Portugal.
15. Weih, N., et al. *Online balancing of a pilot scale fast pyrolysis plant.* in *Proceedings of the 25th European Biomass Conference and Exhibition*. 2017. Stockholm, Sweden.
16. Hoekstra, E., et al., *Heterogeneous and homogeneous reactions of pyrolysis vapors from pine wood.* AIChE Journal, 2012. **58**(9): p. 2830-2842.
17. Funke, A., et al., *Dimensional Analysis of Auger-Type Fast Pyrolysis Reactors.* Energy Technology, 2017. **5**(1): p. 119-129.
18. Funke, A., et al., *Modelling and improvement of heat transfer coefficient in auger type reactors for fast pyrolysis application.* Chemical Engineering and Processing-Process Intensification, 2018. **130**: p. 67-75.

19. Jendoubi, N., et al., *Inorganics distribution in bio oils and char produced by biomass fast pyrolysis: The key role of aerosols.* Journal of Analytical and Applied Pyrolysis, 2011. **92**(1): p. 59-67.
20. Oudenhoven, S.R.G., R.J.M. Westerhof, and S.R.A. Kersten, *Fast pyrolysis of organic acid leached wood, straw, hay and bagasse: Improved oil and sugar yields.* Journal of Analytical and Applied Pyrolysis, 2015. **116**: p. 253-262.
21. Funke, A., et al., *Fast Pyrolysis of Biomass Residues in a Twin-screw Mixing Reactor.* Jove-Journal of Visualized Experiments, 2016(115), e54395.
22. Fahmi, R., et al., *The effect of lignin and inorganic species in biomass on pyrolysis oil yields, quality and stability.* Fuel, 2008. **87**(7): p. 1230-1240.
23. Oasmaa, A., et al., *Controlling the Phase Stability of Biomass Fast Pyrolysis Bio-oils.* Energy & Fuels, 2015. **29**(7): p. 4373-4381.
24. Fonseca, F.G., et al., *Moisture content as a design and operational parameter for fast pyrolysis.* Journal of Analytical and Applied Pyrolysis, 2019. **139**: p. 73-86.
25. Oasmaa, A. and C. Peacocke, *A guide to physical property characterisation of biomass-derived fast pyrolysis liquids.* VTT Publications 2001. **450**: p. 65 pp + app (34 pp).
26. Oasmaa, A., et al., *Pyrolysis Oil Multiphase Behavior and Phase Stability: A Review.* Energy & Fuels, 2016. **30**(8): p. 6179-6200.
27. Funke, A., et al., *Application of fast pyrolysis char in an electric arc furnace.* Fuel Processing Technology, 2018. **174**: p. 61-68.
28. Nicoleit, T., et al., *Particle Shape and Porosity of Biogenic Pyrolysis Char.* Chemie Ingenieur Technik, 2015. **87**(12): p. 1733-1740.
29. Nicoleit, T., N. Dahmen, and J. Sauer, *Production and storage of gasifiable slurries based on flash-pyrolyzed straw.* Energy Technology, 2016. **4**: p. 221.
30. Raffelt, K., et al., *Bio-Slurries From Lignocellulose*, in *Encyclopedia of Sustainable Technologies*, M.A. Abraham, Editor. 2017, Elsevier: Oxford. p. 217-228.
31. Henrich, E., et al., *Fast pyrolysis of lignocellulosics in a twin screw mixer reactor.* Fuel Process. Technol., 2016. **143**: p. 151.
32. Funke, A., et al., *Fast pyrolysis char - Assessment of alternative uses within the bioliq® concept.* Bioresour. Technol., 2016. **200**: p. 905.
33. Niebel, A., et al. *Technical modifications improving operational stability at the bioliq® fast pyrolysis plant*. in *Proceedings of the 26th European Biomass Conference and Exhibition*. 2018. Copenhagen, Denmark.
34. Trippe, F., et al., *Techno-Economic Analysis of Fast Pyrolysis as a Process Step Within Biomass-to-Liquid Fuel Production.* Waste and Biomass Valorization, 2010. **1**(4): p. 415-430.
35. Ille, Y., et al., *Activity of water in pyrolysis oil-Experiments and modelling.* Journal of Analytical and Applied Pyrolysis, 2018. **135**: p. 260-270.